

## Supporting Information

### Self-assembling dendrimer nanotracer for SPECT imaging

Ling Ding, Zhenbin Lyu, Aura Tintaru, Erik Laurini, Domenico Marson, Beatrice Louis, Ahlem Bouhleb, Laure Balasse, Samantha Fernandez, Philippe Garrigue, Eric Mas, Suzanne Giorgio, Sabrina Pricl, Benjamin Guillet, Ling Peng.

### Table of content

<b>Scheme S1</b> .....	<b>3</b>
<b>Figure S1</b> .....	<b>4</b>
<b>Figure S2</b> .....	<b>5</b>
<b>Figure S3</b> .....	<b>6</b>
<b>Figure S4</b> .....	<b>7</b>
<b>General</b> .....	<b>8</b>
<b>Nuclear Magnetic Resonance</b> .....	<b>8</b>
<b>Mass Spectrometry</b> .....	<b>8</b>
<b>Synthesis and characterization of the amphiphilic dendrimer 2</b> .....	<b>9</b>
<b>Synthesis and characterization of the amphiphilic dendrimer In-2</b> .....	<b>9</b>
<b>Critical micelle concentration (CMC)</b> .....	<b>10</b>
<b>Dynamic light scattering (DLS)</b> .....	<b>10</b>
<b>Transmission Electron Microscopy (TEM)</b> .....	<b>10</b>
<b>Isothermal titration calorimetry (ITC)</b> .....	<b>11</b>
<b>Molecular modeling</b> .....	<b>11</b>
<b>Radiolabeling of [<sup>111</sup>In]In-2</b> .....	<b>12</b>
<b>Radiolabeling stability of [<sup>111</sup>In]In-2</b> .....	<b>12</b>
<b>Animals</b> .....	<b>12</b>
<b>Mice orthotopic xenograft models of pancreatic tumors</b> .....	<b>13</b>
<b>SPECT/CT biodistribution and tumor uptake study with [<sup>111</sup>In]In-2</b> .....	<b>13</b>
<b>PET/CT biodistribution and tumor uptake study with [<sup>68</sup>Ga]Ga-1</b> .....	<b>13</b>

<b>Statistics .....</b>	<b>14</b>
<b>Reference .....</b>	<b>14</b>

### Scheme S1: Synthesis of the dendrimers **2** and **In-2**.

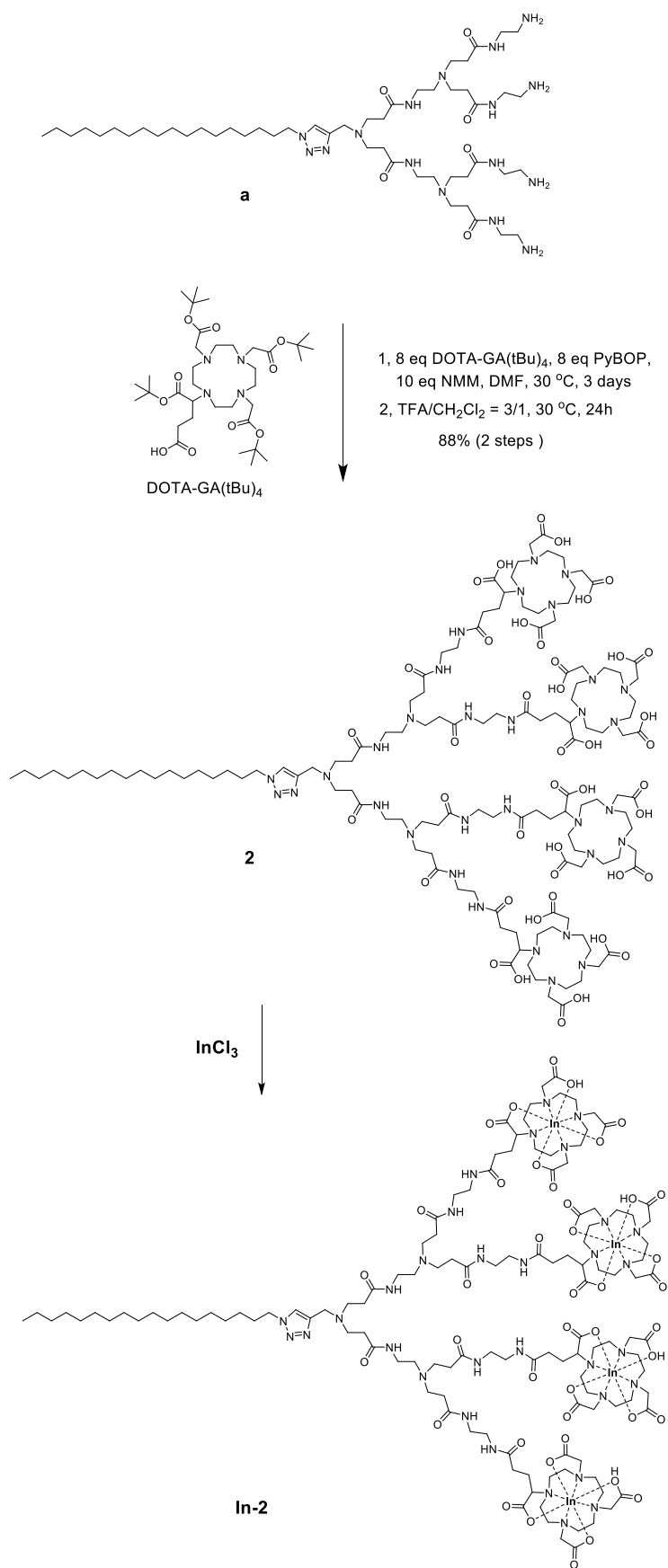


**Figure S1:** (A)  $^1\text{H}$ - and (B)  $^{13}\text{C}$ -NMR spectra of the DOTA-conjugated dendrimer **2** recorded in  $\text{D}_2\text{O}$  at 300K.

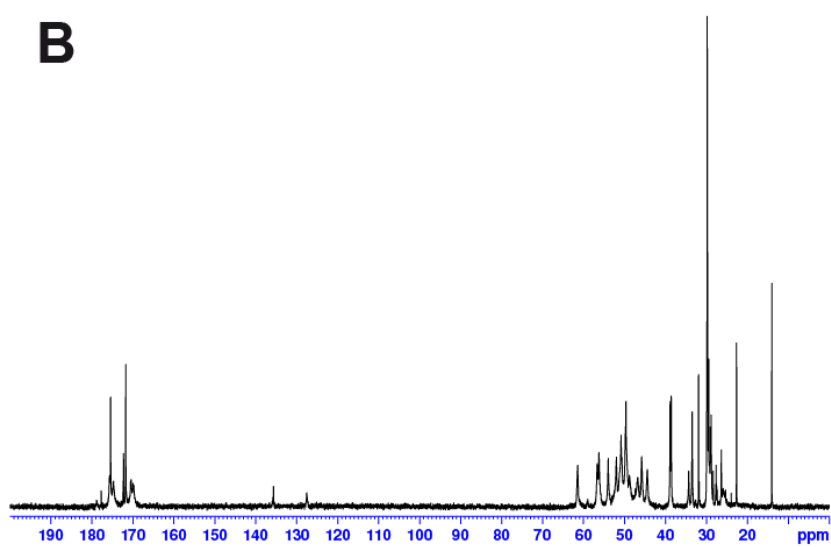
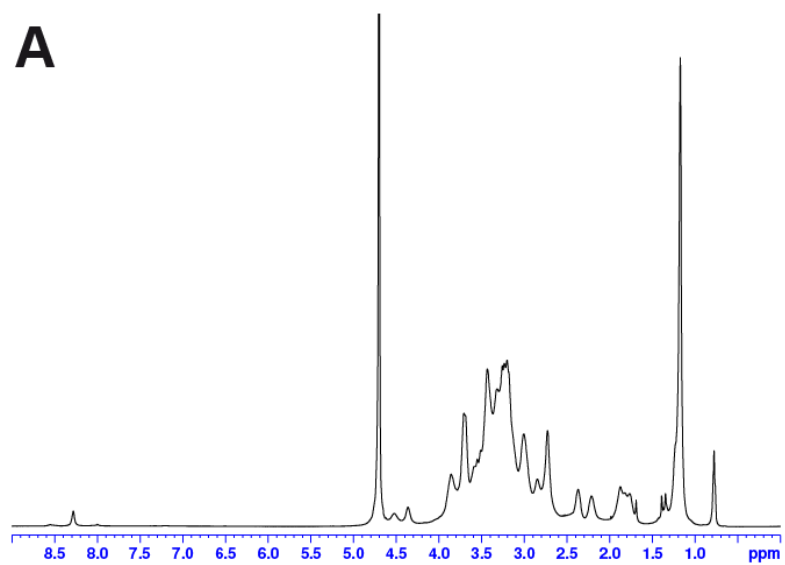


**Figure S2:** (A)  $^1\text{H}$ - $^{13}\text{C}$  HSQC spectrum of DOTA-conjugated dendrimer **2**, recorded at 300K in  $\text{D}_2\text{O}$ . (B) The enlarged region of the HSQC spectrum.

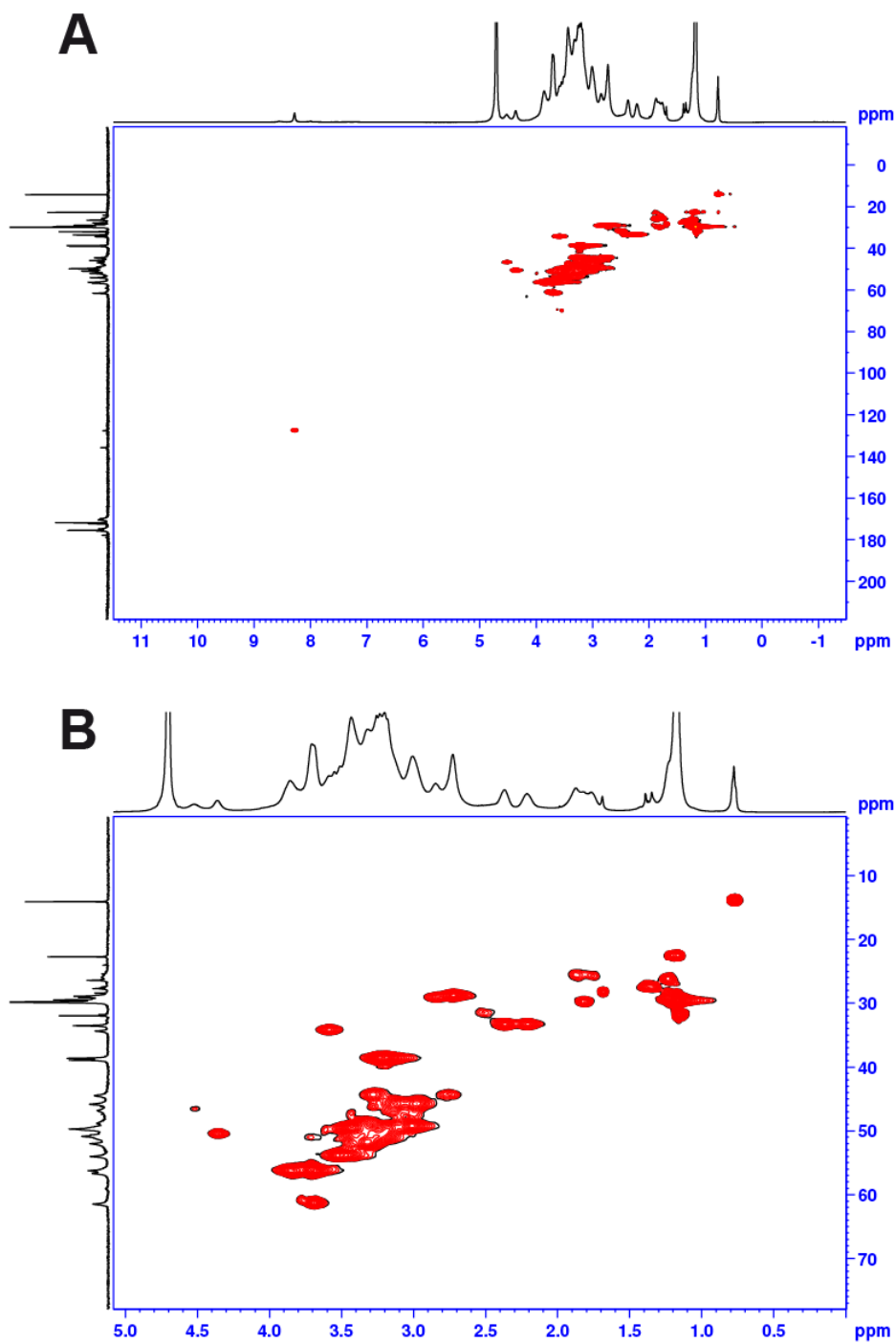


**Figure S3:** High-resolution ESI(+)-MS spectrum of (A) **2** and (B) **In-2** recorded in acidified methanol.

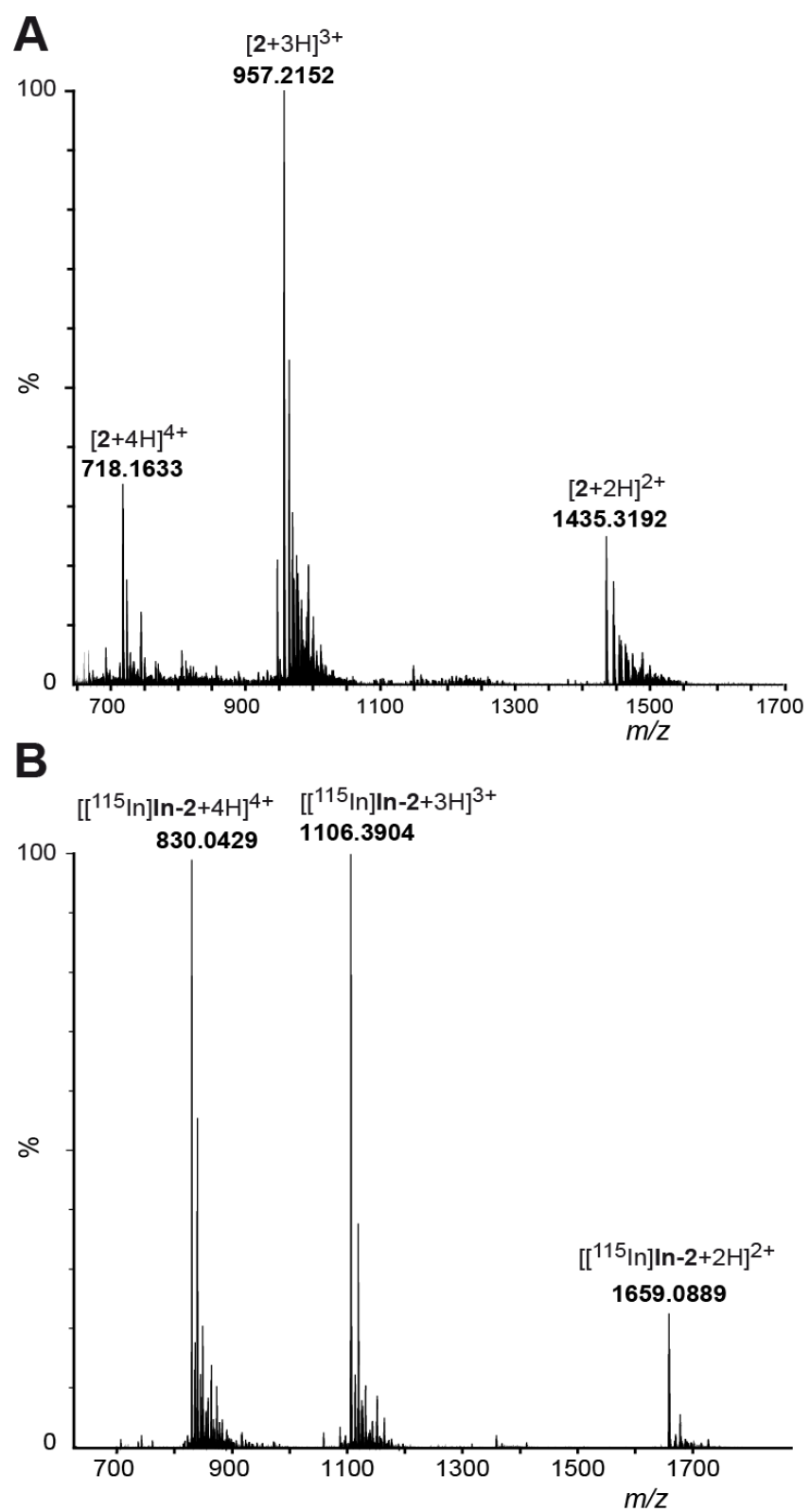
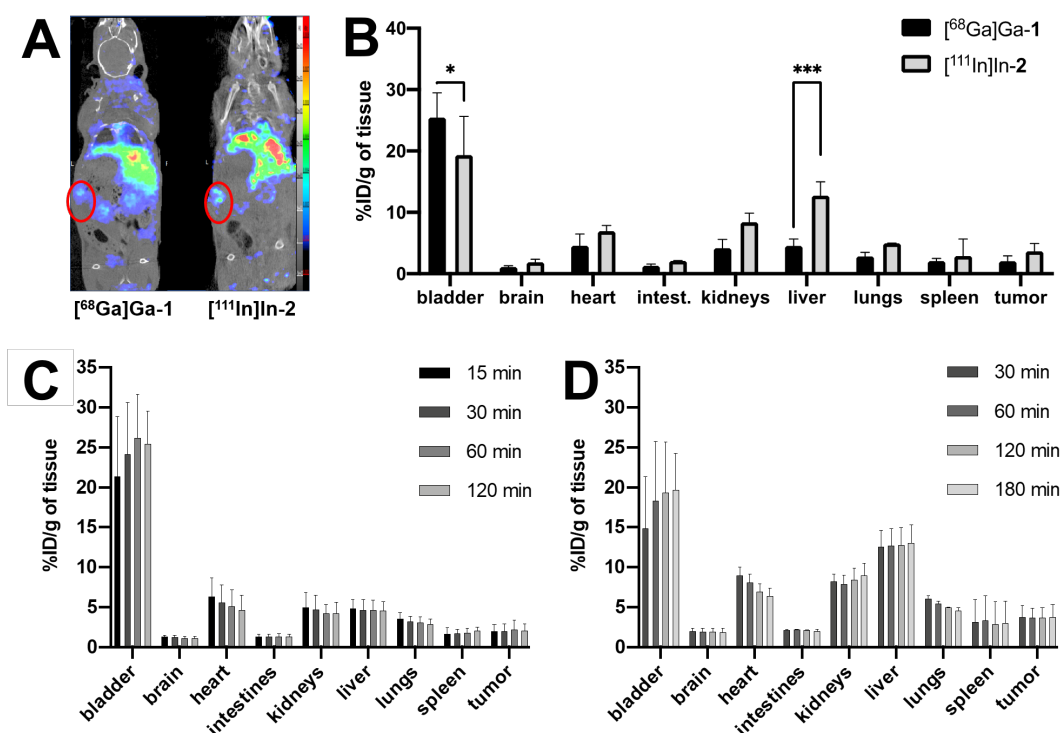


**Figure S4:** Comparison of radiolabeled dendrimer [<sup>68</sup>Ga]Ga-1 for PET imaging and [<sup>111</sup>In]In-2 for SPECT imaging in a mouse orthotopic xenograft model of pancreatic adenocarcinoma (SOJ-6 cell line). (A) Representative μPET/CT image of [<sup>68</sup>Ga]Ga-1 (left) and μSPECT/CT image of [<sup>111</sup>In]In-2 (right) 120 minutes after intravenous injection. Orthotopic SOJ-6 tumors are highlighted by the red circles (n=3 mice). (B) Biodistribution of [<sup>68</sup>Ga]Ga-1 and [<sup>111</sup>In]In-2 quantified in each organ by μPET/CT and μSPECT/CT respectively 120 min after injection. Results are expressed as the mean percentage of injected dose per gram of tissue (n=3 mice). The two compounds show significantly different biodistributions overall (2-way ANOVA \*\*P=0.0071). Sidak's multiple comparison found that the [<sup>111</sup>In]In-2 signal was significantly higher in the liver (\*\*\*P=0.0003) and significantly lower in the bladder (\*P=0.0110). (C) Biodistribution of [<sup>68</sup>Ga]Ga-1 quantified in each organ by dynamic μPET/CT up to 120 min after injection. Results are expressed as the mean percentage of injected dose per gram of tissue (n=3 mice). (D) Biodistribution of [<sup>111</sup>In]In-2 quantified in each organ by dynamic μSPECT/CT up to 180 min after injection. Results are expressed as the mean percentage of injected dose per gram of tissue (n=3 mice).



## General

The starting material of the amine-terminated dendrimer was synthesized according to the well-established protocol published in our group.<sup>1</sup> DOTA-GA(tBu)<sub>4</sub> and NODA-GA(tBu)<sub>3</sub> were purchased from CheMatech (Dijon, France). Other chemicals were purchased from Acros Organics, Sigma Aldrich or Alfa Aesar. Dialysis tubing was purchased from Sigma Aldrich (St. Quentin Fallavier, France). Radiolabeling analyses were performed on instant thin layer chromatography (iTLC) with a MiniGITA radiochromatography system (Elisia-Raytest, Angleur, Belgium).

## Nuclear Magnetic Resonance

Nuclear Magnetic Resonance (NMR) experiments were acquired in D<sub>2</sub>O (EuroIsotop, Saint Aubin, France), at 300K using a Bruker Avance DRX 500 NMR spectrometer (Karlsruhe, Germany) operating at 500.13 MHz for <sup>1</sup>H and 125.77 MHz for <sup>13</sup>C Larmor frequency with a double resonance broadband fluorine observe (BBFO) 5 mm probe head. <sup>13</sup>C-NMR experiments were recorded using one-pulse excitation pulse sequence (90° excitation pulse) with <sup>1</sup>H decoupling during signal acquisition (performed with WALTZ-16); the relaxation delay has been set at 2 s. For each analyzed sample, depending on the compound concentration, 3k up to 5k free induction decays (FID) 64k complex data points were collected using a spectral width of 30000 Hz (240 ppm). Chemical shifts (δ in ppm) were reported relative to residual signal of CDCl<sub>3</sub> (δ<sub>C</sub> 77.04 ppm). Complete <sup>1</sup>H and <sup>13</sup>C assignments of the new compound were obtained using 2D gradient-selected NMR experiments, <sup>1</sup>H-<sup>1</sup>H COSY (COrrrelation SpectroscopY), <sup>1</sup>H-<sup>13</sup>C HSQC (Heteronuclear Single Quantum Correlation), <sup>1</sup>H-<sup>13</sup>C HMBC (Heteronuclear Multiple Bond Coherence) and <sup>1</sup>H-<sup>1</sup>H NOESY (Nuclear Overhauser Effect SpectroscopY), for which conventional acquisition parameters were used, as described in the literature.<sup>2</sup>

## Mass Spectrometry

High resolution mass spectrometry experiments were performed with a Synapt G2 HDMS quadrupole/time-of-flight (Manchester, UK) equipped with an electrospray

source operating in positive mode. Samples were introduced at 10  $\mu\text{L}/\text{min}$  flow rate (capillary voltage +2.8 kV, sampling cone voltage: varied between +20 V and +60 V) under a curtain gas ( $\text{N}_2$ ) flow of 100 L/h heated at 35  $^\circ\text{C}$ . Accurate mass experiments were performed using reference ions from  $\text{CH}_3\text{COONa}$  internal or external standard. The samples were dissolved and further diluted in methanol (Sigma-Aldrich, St-Louis - MO, USA) doped with formic acid (1% v/v) prior to analysis. Data analyses were conducted using MassLynx 4.1 programs provided by Waters.

### **Synthesis and characterization of the amphiphilic dendrimer 2**

To a solution of DOTA-GA(*t*Bu)<sub>4</sub> (162 mg, 23  $\mu\text{mol}$ ) in DMF (3.0 mL) were added PyBOP (121 mg, 232  $\mu\text{mol}$ ) and NMM (29 mg, 290  $\mu\text{mol}$ ). The mixture was stirred for 5.0 min and then a solution of the amine-terminating dendrimer (30 mg, 29  $\mu\text{mol}$ ) in DMF (2.0 mL) was added, and the resulting solution was stirred at 30  $^\circ\text{C}$  for 3.0 days under argon. Then, a saturated  $\text{NaHCO}_3$  solution (15 mL) was added to the reaction mixture and ethyl acetate ( $3 \times 15$  mL) was used for extraction of the synthesized product. The combined organic layers were collected, dried over anhydrous  $\text{MgSO}_4$ , filtrated and evaporated under reduced pressure. The crude material was used without any purification for the next step. It was dissolved in a TFA/ $\text{CH}_2\text{Cl}_2$  mixture (3.0 mL, v/v = 3/1) and stirred at 30  $^\circ\text{C}$  for 24 h under argon. After evaporating the solvent, the crude residue was purified by dialysis (dialysis tubing, MWCO 2000) and lyophilized.<sup>3</sup> Repeating the operation of dialysis and lyophilization 7 times, the product was lyophilized to yield the corresponding **2** as a white solid (73 mg, yield: 88%). <sup>1</sup>H NMR (500 MHz,  $\text{D}_2\text{O}$ ):  $\delta$  8.27 (s, 1H), 4.50 (br, 2H), 4.34 (br, 2H) 3.83-2.70 (m, 138H), 2.34 (br, 4H), 2.18 (br, 4H), 1.86 (br, 12H), 1.15 (br, 30H), 0.75 (s, 3H); <sup>13</sup>C NMR (100 MHz,  $\text{D}_2\text{O}$ )  $\delta$  176.5, 175.3, 173.4, 172.4, 171.7, 135.8, 127.5, 66.3, 57.8, 51.3, 49.7, 47.1, 46.9, 38.9, 38.5, 36.5, 32.8, 32.0, 29.9, 29.5, 29.1, 28.8, 27.8, 26.4, 24.8, 22.7, 14.1. ESI(+)-HRMS: calculated isotopic maximum for  $\text{C}_{127}\text{H}_{226}\text{N}_{32}\text{O}_{42}^{4+}$   $m/z$  718.1634; found at  $m/z$  .718.1633 (error: -0.1 ppm).

### **Synthesis and characterization of the amphiphilic dendrimer In-2**

The dendrimer **2** (2.5 mg, 0.9  $\mu\text{mol}$ ) was dissolved in 2.0 mL  $\text{H}_2\text{O}$ . To this solution was added the solution of  $\text{InCl}_3$  (0.85 mg, 3.8  $\mu\text{mol}$ ) in 0.1M HCl and the pH value was adjusted to 5.0 with addition of 0.2 M ammonium acetate. The mixture was stirred for 2 h at 37 °C under Argon. The obtained crude product was purified by dialysis (dialysis tubing, MWCO 2000) and lyophilized to yield the corresponding **In-2** as a white solid (2.5 mg, yield: 87%). ESI(+)-HRMS: calculated isotopic maximum at  $m/z$  1106.3896 for  $\text{C}_{127}\text{H}_{213}\text{N}_{32}\text{O}_{42}\text{In}_4^{3+}$ ; found at  $m/z$  1106.3904 (error: +0.7 ppm).

### **Critical micelle concentration (CMC)**

CMC was determined using Nile red as a fluorescence probe. Dendrimer **In-2** solutions at different concentrations varied from  $1.0 \times 10^{-7}$  to  $2.00 \times 10^{-4}$  mol/L were prepared and the final Nile red concentration was  $3 \times 10^{-6}$  mol/L in water. The solutions were vortexed for 10 min and kept for 2 h at room temperature to promote the micelle formation prior to fluorescence measurement. Fluorescence spectra were recorded at the emission wavelength of 635 nm on F-4500 fluorescence spectrophotometer at room temperature. Excitation wavelength is 550 nm. The normalized fluorescence intensity was analyzed as a function of micelle concentration.

### **Dynamic light scattering (DLS)**

Dynamic light scattering (DLS) measurements were performed to determine the hydrodynamic diameter and zeta potential of the nanoparticles formed with **In-2**. The dendrimer **In-2** was first dispersed in MilliQ water at a concentration of 0.5 mg/mL, and sonicated 30 seconds at 60 Hz (Ultrasonic Cleaner Branson B-200), then the fresh solution was measured using a Malvern Zetasizer Nano ZS equipped with a standard 633 nm laser at 25 °C. The experiments were done in triplicates.

### **Transmission Electron Microscopy (TEM)**

Transmission electron microscopy (TEM) was performed using JEOL 3010F analytical electron microscope (Tokyo, Japan) to characterize the size and morphology of the NPs

at an accelerating voltage of 300 kV. The dendrimer **In-2** was dispersed in milliQ water at a concentration of 1.0 mg/mL, and sonicated for 30 seconds, then diluted to 1.6  $\mu\text{g/mL}$ , followed by depositing an aliquot (4.0  $\mu\text{L}$ ) onto a carbon-coated copper grid and dried at 37 °C. The grid was then stained with 3.0  $\mu\text{L}$  uranyl acetate (2.0 % in aqueous solution) for 4 seconds, and the excess uranyl acetate was removed by filter paper before measurements.

### **Isothermal titration calorimetry (ITC)**

Isothermal titration calorimetry (ITC) experiments were performed with a MicroCal PEAQ-ITC calorimeter (Malvern, UK) at 37°C. The cell volume was 208  $\mu\text{L}$ . The thermodynamic parameters for the formation of the **In-2** complex was investigated in buffered solutions at pH = 5.0. Specifically, a solution of the dendrimer **2** at concentration of 100  $\mu\text{M}$  (above its CMC) was titrated with 19 step-by-step injections (interval = 150 s) of 2  $\mu\text{L}$  volume of a solution of  $\text{InCl}_3$  (in syringe) at the concentration of 4000  $\mu\text{M}$ . All solutions and buffer were degassed for 30 min at room temperature under stirring at 600 rpm prior to each experiment. After careful washing, the cell was pre-rinsed with a portion of the buffer solutions. Upon filling cell and syringe, stirring was turned on and the system was allowed to thermally equilibrate for 30 minutes. The values of unspecific heats due to dilution effects and liquid friction were further confirmed by control experiments (data not shown); accordingly, they were subtracted from the relevant data set to yield the corrected integrated data. All experiments were run in triplicates.

### **Molecular modeling**

**In-2** atom types were assigned via the Generalized Amber Force Field (GAFF)<sup>4</sup> and the Visual Force Field Derivation Toolkit (VFFDT).<sup>5</sup> 100 monomers of **In-2** were randomly placed in a simulation cubic box filled with TIP3 waters<sup>6</sup> and extending at least 20 Å nm from each solute molecule. Then, the required amount of  $\text{Cl}^-$  ions were added to neutralize the system, removing eventual overlapping water molecules. The solvated **In-2** molecules were subjected to a combination of steepest descent/conjugate

gradient minimisation of the potential energy, during which all bad contacts were relieved. Next, the optimized structure was gradually heated and relaxed to 298 K by running 500 ps of molecular dynamics (MD) simulations in the canonical (NVT) ensemble under periodic boundary condition. The SHAKE algorithm<sup>7</sup> was applied to all covalent bonds involving hydrogen atoms. For temperature regulation the Langevin thermostat<sup>8</sup> was adopted and an integration time step of 2 fs was applied. The final heating step was followed by 100 ns of MD equilibration in the isochoric/isothermal (NPT) ensemble. Pressure control was exerted by coupling the system to a Berendsen barostat (pressure relaxation time 2 ps).<sup>7</sup> The Particle Mesh Ewald (PME) method<sup>9</sup> was used to treat the system electrostatics with a direct space cut-off of 10 Å. Finally, the NPT MD production run was performed for another 1000 ns. In this case, the Monte Carlo barostat implemented in Amber 18 was adopted for pressure control (1 bar). All simulations were carried out using AMBER 18<sup>10</sup> on a CPU/GPU hybrid cluster.

### **Radiolabeling of [<sup>111</sup>In]In-2**

0.035 mL of 0.2 M ammonium acetate solution was added to 0.025 mL dendrimer solution of **2** (1.0 mg/mL in milliQ water). To this solution was added 0.035 mL of [<sup>111</sup>In]InCl<sub>3</sub> solution ordered from Curium (Saclay, France). The resulting solution at pH = 5 was heated at 58°C for 14 min and then vortexed to promote the spontaneous self-assembly of [<sup>111</sup>In]In-**2**. The radiochemical purity of 91% was determined by iTLC (solid phase: iTLC-SG paper purchased from Agilent (Les Ulis, France), mobile phase: 0.10 M sodium citrate pH = 5.0). The solution was used for *in vitro* and *in vivo* studies without further purification.

### **Radiolabeling stability of [<sup>111</sup>In]In-2**

The radiolabeling stability of [<sup>111</sup>In]In-**2** was assessed by incubating 0.10 mL of the radiotracer solution in 0.40 mL of human serum at 37°C. The radiochemical purity stability was checked by iTLC, 1h, 2h and 30h after the radiosynthesis.

### **Animals**

All procedures using animals were approved by the Institutional Animal Care and Use Committee (CE14, Aix-Marseille University) and were conducted according to the EU Directive 2010/63/EU. Six-week-old athymic nude mice were purchased from Envigo. Animals were housed in enriched cages placed in a temperature- and hygrometry-controlled room with daily monitoring, fed with water and commercial diet *ad libitum*.

### **Mice orthotopic xenograft models of pancreatic tumors**

$10^7$  trypsinized SOJ-6 (primary pancreatic adenocarcinoma) cells were resuspended in 0.25 mL Roswell Park Memorial Institute (RPMI) 1640 culture media (ThermoFisher Scientific, Waltham, USA) with 10% fetal calf serum and 0.25 mL Matrigel Matrix (Corning, New York, USA). Each mouse was injected with  $10^6$  SOJ-6 cells/50  $\mu$ L in the pancreas. Animals were allowed for resting during 3 weeks.

### **SPECT/CT biodistribution and tumor uptake study with [ $^{111}\text{In}$ ]In-2**

Mice were injected in the caudal vein with  $1.9 \pm 0.2$  MBq of [ $^{111}\text{In}$ ]In-2 and immediately imaged for a 3 hour-long dynamic SPECT/CT on a NanoSPECT/CT camera (Mediso, Budapest, Hungary) under 1.5% isoflurane anesthesia. Reconstruction and image treatment were carried out with InvivoSPECT software (Invicro, Boston, USA) to assess tracer uptake in liver, heart, lungs, kidneys, bladder, brain, intestines, forelimb *triceps brachii* muscle, spleen and SOJ6 tumor, 30, 60, 120 and 180 minutes after injection. Results were expressed as mean  $\pm$  sd percentage of the injected dose per gram of tissue (%ID/g).

### **PET/CT biodistribution and tumor uptake study with [ $^{68}\text{Ga}$ ]Ga-1**

[ $^{68}\text{Ga}$ ]Ga-1 was prepared as previously described<sup>3</sup> and was injected to the same mice 2 days before [ $^{111}\text{In}$ ]In-2 injection. Reconstruction and image treatment of the dynamic PET were carried out with Vivoquant<sup>®</sup> software (Invicro, Boston, USA) to assess tracer uptake in liver, heart, lungs, kidneys, bladder, brain, intestines, forelimb *triceps brachii* muscle, spleen and SOJ6 tumor, 30, 60, and 120 minutes after injection. Results were expressed as mean  $\pm$  sd percentage of the injected dose per gram of tissue (%ID/g).

## Statistics

Radiochemical purities were compared with 1-way ANOVA followed by a post-hoc Bonferroni test. Tumor uptakes were compared with rank-signed Wilcoxon t-test. Statistical analyses were performed with Prism<sup>®</sup> software (GraphPad Software).  $P \leq 0.05$  indicated statistical significance

## Reference

1. T. Yu, X. Liu, A.-L. Bolcato-Bellemin, Y. Wang, C. Liu, P. Erbacher, F. Qu, P. Rocchi, J.-P. Behr and L. Peng, *Angewandte Chemie International Edition*, 2012, **51**, 8478-8484.
2. S. Braun, H.-O. Kalinowski and S. Berger, *150 and more basic NMR experiments: a practical course*, Wiley-Vch, 1998.
3. P. Garrigue, J. Tang, L. Ding, A. Bouhlef, A. Tintaru, E. Laurini, Y. Huang, Z. Lyu, M. Zhang, S. Fernandez, L. Balasse, W. Lan, E. Mas, D. Marson, Y. Weng, X. Liu, S. Giorgio, J. Iovanna, S. Pricl, B. Guillet and L. Peng, *Proceedings of the National Academy of Sciences*, 2018, **115**, 11454-11459.
4. J. Wang, R. M. Wolf, J. W. Caldwell, P. A. Kollman and D. A. Case, *Journal of Computational Chemistry*, 2004, **25**, 1157-1174.
5. S. Zheng, Q. Tang, J. He, S. Du, S. Xu, C. Wang, Y. Xu and F. Lin, *Journal of Chemical Information and Modeling*, 2016, **56**, 811-818.
6. W. L. Jorgensen, J. Chandrasekhar, J. D. Madura, R. W. Impey and M. L. Klein, *The Journal of Chemical Physics*, 1983, **79**, 926-935.
7. J.-P. Ryckaert, G. Ciccotti and H. J. C. Berendsen, *Journal of Computational Physics*, 1977, **23**, 327-341.
8. X. Wu and B. R. Brooks, *Chemical Physics Letters*, 2003, **381**, 512-518.
9. T. Darden, D. York and L. Pedersen, *The Journal of Chemical Physics*, 1993, **98**, 10089-10092.
10. D. A. Case, I. Y. Ben-Shalom, S. R. Brozell, D. S. Cerutti, T. E. Cheatham III, V. W. D. Cruzeiro, T. A. Darden, R. E. Duke, D. Ghoreishi, M. K. Gilson, H. Gohlke, A. W. Goetz, D. Greene, R. Harris, N. Homeyer, S. Izadi, A. Kovalenko, T. Kurtzman, T. S. Lee, S. LeGrand, P. Li, C. Lin, J. Liu, T. Luchko, R. Luo, D. J. Mermelstein, K. M. Merz, Y. Miao, G. Monard, C. Nguyen, H. Nguyen, I. Omelyan, A. Onufriev, F. Pan, R. Qi, D. R. Roe, A. Roitberg, C. Sagui, S. Schott-Verdugo, J. Shen, C. L. Simmerling, J. Smith, R. Salomon-Ferrer, J. Swails, R. C. Walker, J. Wang, H. Wei, R. M. Wolf, X. Wu, L. Xiao, D. M. York and P. A. Kollman, *University of California, San Francisco*.